R&D NOTE

Microfluidic Y-Junctions: A Robust Emulsification System with Regard to Junction Design

Maartje L. J. Steegmans, Karin G. P. H. Schroën, and Remko M. Boom
Food Engineering Group, Dept. ATV, Wageningen University, P.O. Box 8129, 6700 EV Wageningen, The Netherlands

DOI 10.1002/aic.12094
Published online January 4, 2010 in Wiley InterScience (www.interscience.wiley.com).

Keywords: emulsion, microdevice, drop, T-junction, Y-junction

Introduction

Many microfluidic devices have been suggested for emulsification. One of the most studied designs is the T-junction.[1,2,3,4,5,6]. Also Y-junctions are reported,[7,8,9,10] and although they basically seem to be odd-shaped T-junctions, no systematic investigation has yet been carried out regarding the design, and how this relates to the droplet size that can be produced. Therefore, we experimentally investigated the effect of microfluidic (flat) Y-junction design on emulsion droplet size in the dripping and jetting regime for a hexadecane/ethanol-water model system with a range of static interfacial tensions and continuous-phase viscosities, and compared these to results obtained for T-junctions. It is expected that the droplet size in T-junctions, which is known to consist of two steps,[14] will differ from that in Y-junctions, which in a previous study based on a single Y-junction design was found to scale linearly with the capillary number of the continuous phase, implying a one-step droplet-formation process.[10]

Experimental

Materials

Anhydrous n-hexadecane (no. 296317, Sigma-Aldrich, Steinheim, Germany) was used as the to-be-dispersed-phase. Milli-Q water, 9, 19, 28, 38, 47, or 66 wt % ethanol-water mixtures were prepared from Milli-Q water and 96%v/v ethanol (no. 20824, VWR BDH Prolabo, Amsterdam, The Netherlands), and were used as continuous phases. The viscosity of these Newtonian liquids was measured in a rheometer (MCR 301, Anton Paar, Graz, Austria) with a Couette geometry (DG 26.7, Anton Paar, Graz, Austria) (see Table 1). The interfacial tension with hexadecane was measured using a dynamic drop tensiometer (ADT, ITCONCEPT, Longessaigne, France)[10,11] (see Table 1).

Experimental setup

Microfluidic Devices. Borosilicate glass microfluidic devices with various Y- and T-junction designs were produced by Micronit Microfluidics BV (Enschede, The Netherlands) (see Figure 1 and Table 2). The devices consist of a plate in which the channels are (chemically) etched, and annealed to a top plate with inlets. The microchannels have a uniform depth of 5 μm and are much wider than deep. The continuous phase enters the junction via *C*, and the hexadecane via *HD*. At the junction, both phases meet and hexadecane droplets are formed (see for instance Figure 3a).

Droplet-Formation Experiments. The microfluidic devices were operated in the appropriate holder (no. 4515, Micronit Microfluidics BV, Enschede, The Netherlands), and the continuous phase and the hexadecane were supplied as described in previous work.[10,12] At continuous-phase flow rates ranging from 0.014 to 0.44 $mL \cdot h^{-1}$ and hexadecane flow rates ranging from 0.29 to 13 $\mu L \cdot h^{-1}$ droplets were formed at the junctions (flow rates were estimated as described in previous work[10]). After setting the flow rate(s), droplet formation was allowed to equilibrate for at least two min to ensure steady state.

Droplet formation was recorded using a high-speed camera (MotionPro HS-4, Redlake, Tallahassee, FL) connected to an inverted transmitted light microscope (Axiovert 200, Carl Zeiss, Sliedrecht, The Netherlands). The formation of

Additional Supporting Information may be found in the online version of this article.

Correspondence concerning this article should be addressed to M. L. J. Steegmans at maartje.steegmans@wur.nl

Table 1. Viscosity η and Interfacial Tension with Hexadecane γ_{HD} at 23°C

Sample	η [mPa·s]	γ_{HD} [mN·m^{-1}]
Milli-Q water	1.0	41
9 wt.% ethanol-water	1.5	27
19 wt.% ethanol-water	2.0	20
28 wt.% ethanol-water	2.5	15
38 wt.% ethanol-water	2.6	12
47 wt.% ethanol-water	2.7	10
66 wt.% ethanol-water	2.3	7
Hexadecane	3.5	–

25 subsequent hexadecane droplets was recorded using (ca.) 20 frames per droplet, which corresponds to frame rates between 500 and 94,500 s^{-1}.

Image analysis

Droplet Size. The hexadecane droplet size was determined either automatically using a custom-written script based on the DIPimage toolbox operating in Matlab 7.0.1, or manually using Image-Pro Plus 4.5.0.29 when image contrast was too low. The area of each droplet was determined as the average over three subsequent frames. Ten subsequent droplets were measured; the reported size was the average of these 10 with a 95% confidence interval.

The droplet volume V was calculated from the droplet area. When the diameter of the droplet was smaller than the depth of the microchannel, the droplet was spherical (drop); otherwise, the droplet was squeezed between the bottom and top surface and disc-shaped (disc). The volume V of discs was calculated assuming rounded edges with the channel depth as curvature

$$V = \frac{\pi z}{4}(D - z)^2 + \frac{\pi^2 z^2}{8}\left(D - \left(1 - \frac{4}{3\pi}\right)z\right) \quad (\mathrm{m}^3), \qquad (1)$$

with D the diameter of the disc area, and z the depth of the microchannels. To compare drops and discs, the equivalent dia. D_{3D} of an unrestricted spherical droplet was calculated.

Neck Diameter. Just before detachment the droplet is kept to the bulk with a hexadecane filament, which thinnest width D_{neck} was manually determined with Image-Pro Plus 4.5.0.29 in the second-to-last frame before droplet detachment (see Figure 3a and b). The reported D_{neck} is the average over 10 incipient droplets, and the error due to image analysis is 0.8 μm, at most.

Results and Discussion

In previous work [10] on Y-junctions, we found that the droplet-size scales with the inverse square root of the capillary number of the continuous phase $\mathrm{Ca_c}$.[†] Figure 2 shows the data accordingly. For all Y-geometries the droplet size increases (seemingly linearly) with the inverse square root of Ca_c; i.e., as expected droplet size increases with increasing interfacial tension and decreasing continuous-phase velocity.[8,10] Surprisingly, no differences are observed between the various Y-junction designs, which suggests that droplet size, and, therefore, droplet formation mechanism are not influenced by the junction angle, or the length of the various channels; this is in line with our visual observations. In contrast, for droplets formed at, what we expect are, wider Y-junctions with smaller angles than investigated here, Kawai et al.[8] found a decrease in droplet size with increasing angle.

Figure 2 shows that droplets generated at T-junctions are generally larger than at Y-junctions and show more scatter. This is caused by the fact that both continuous- and disperse-phase flow rate determine droplet size at T-junctions,[13] in agreement to the fact that droplet formation is described by a two-step model.[14] In contrast, at Y-junctions, droplet size is independent of the disperse-phase flow rate and droplet size is described by an one-step model as can be deduced from the dependency of the capillary number.[10] In previous work on T-junctions,[14] droplet-size data from various literatures on emulsification at microfluidic T-junctions (with a uniform depth) were statistically investigated, and it was found that the data can be described with a two-step model regardless of the fact that the channels were of equal or different width. Therefore, it is safe to assume that the difference found between T- and Y-junctions is not related to the difference in channel width, and that Y-junctions are not just a variant of T-junctions, as is often assumed. Given the straightforward scaling relation through the capillary number, Y-junctions are the preferred option for small monodisperse emulsion droplets.

The neck diameter just before detachment also seems hardly influenced by the Y-geometry. When compared to T-junctions, the neck in Y-junctions is mostly smaller; but if they are equal the droplets formed at T-junctions are larger (see Figure 3c). This may suggest that Y-junctions facilitate deformation of the hexadecane filament resulting in faster collapse of the neck, and this could explain the difference in

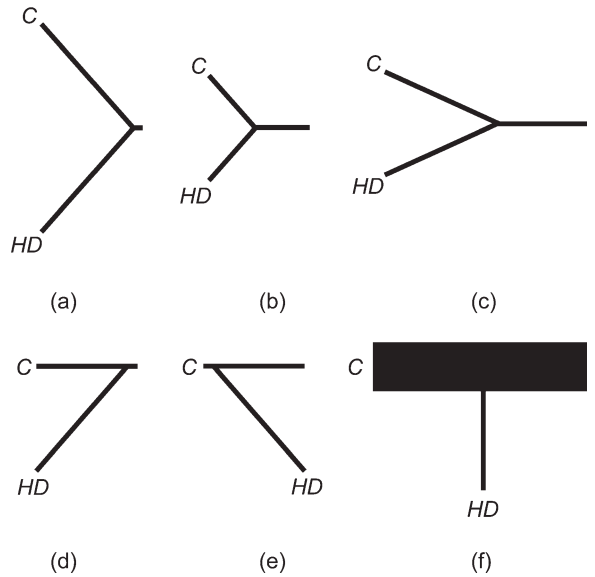

Figure 1. Y- (a–e), and T-junction (f), designs studied, *C* is the continuous-phase channel, HD the hexadecane channel, and at the junction between *C* and *HD* droplets are formed.

[†]Capillary number of the continuous phase is defined as $Ca_c = \eta_c v_c / \gamma_{HD}$, with η_c and v_c the dynamic viscosity and the velocity of the continuous phase, respectively, and γ_{HD} the interfacial tension.

Table 2. Angle at the Junction, Length L and Width w of the Continuous-phase channel C, the Hexadecane Channel HD, and the Downstream Channel for the Designs Shown in Figure 1

Geometry	Angle [°]	L_c [mm]	w_c[a] [μm]	L_{HD} [mm]	w_{HD}[a] [μm]	$L_{\text{downstream}}$ [mm]	$w_{\text{downstream}}$[a] [μm]
a.1	97	6.66	23.0 ± 0.4	6.66	23.2 ± 0.4	0.46	23.0 ± 0.5
a.2	97	6.66	18.0 ± 0.5	6.66	18.3 ± 0.5	0.46	18.2 ± 0.5
b	97	3.36	18.4 ± 0.8	3.36	18.3 ± 0.8	2.66	18.3 ± 0.8
c	49	6.04	18.1 ± 0.8	6.04	18.7 ± 0.8	4.40	18.2 ± 0.8
d	49	4.40	18.0 ± 0.8	6.66	18.4 ± 0.8	0.46	18.0 ± 0.8
e	131	0.46	19.0 ± 0.5	6.66	19.3 ± 0.7	4.40	18.8 ± 0.5
f	90	5.13	303 ± 0.8	4.8	24 ± 0.8	5.13	303 ± 0.8

[a]Widths are given with their 95% confidence interval (average ± 1.96·standard deviation).

the observed droplet size because of a difference in droplet formation process.

Figure 3c shows that for Y-junctions the droplet size is proportional to the diameter of the neck, which is expected assuming a force balance between the shear force and the interfacial tension force acting on the circumference of the

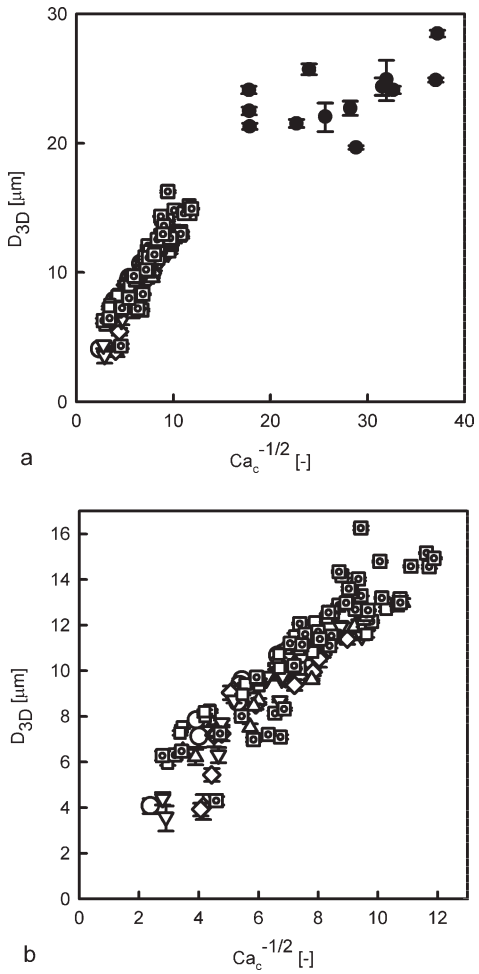

Figure 2. Droplet size D_{3D} as function of the inverse square root of the capillary number of the continuous phase $Ca_c^{-1/2}$ for Y-junctions a.1 (⊡), a.2 (□), b (○), c (◇), d (▽), and e (△), and T-junction f (●) at various flow rates and for various ethanol-water phases.

Figure 2b is an enlargement; the error bars are 95% confidence intervals.

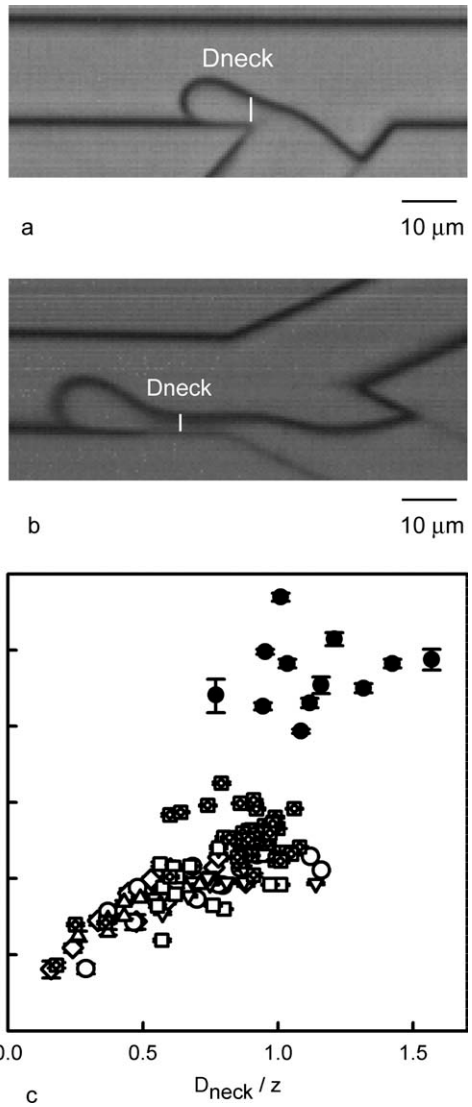

Figure 3. Picture of the neck in a geometry e: hexadecane-in-19 wt % ethanol-water (ϕ_c = 6.2·10^{-2} mL·h^{-1}, ϕ_d = 9.6·10^{-4} mL·h^{-1}), and b. geometry c: hexadecane-in-9 wt % ethanol-water (ϕ_c = 0.10 mL·h^{-1}, ϕ_d = 3.2·10^{-3} mL·h^{-1}). c. dimensionless droplet size D_{3D}/z as function of the dimensionless neck diameter. D_{neck}/z for Y-junctions a.1 (⊡), a.2 (□), b (○), c (◇), d (▽), e (△), and T- junction f (●) at various flow rates and for various ethanol-water phases. The error bars represent the 95% confidence intervals.

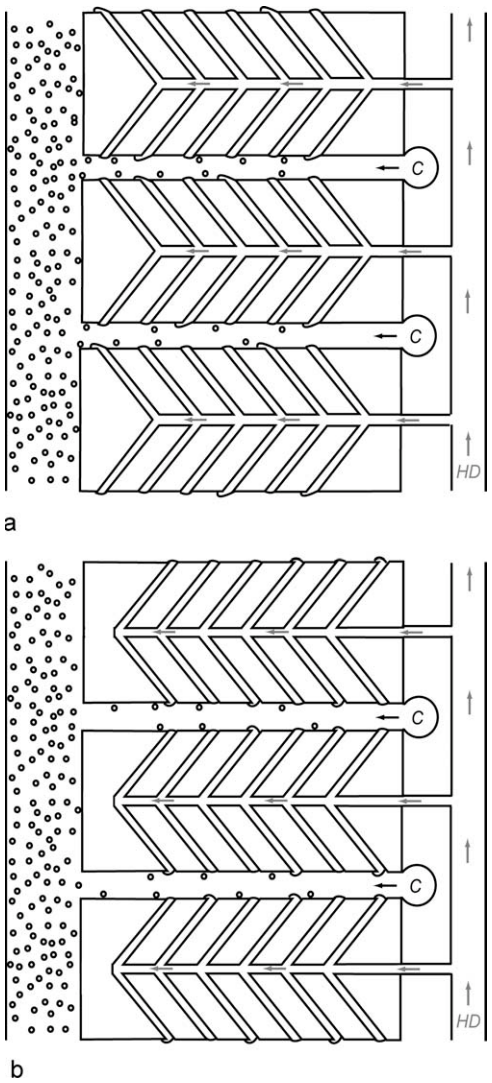

Figure 4. Outline of possible mass-parallelization of Y-junction design d (a.) and e (b.). *C* represents the inlet of the continuous-phase channel and HD the inlet of the hexadecane channel.

Dimensions are not to scale.

neck.[10] Combination of Figures 2 and 3c (result not explicitly shown) suggests that the neck diameter is proportional to Ca_c^{-1}; which implies that the interfacial tension, continuous-phase velocity, and viscosity determine the size of the neck, and, therefore, the size of the droplet.

There is a great demand for micron-sized, monodisperse emulsion droplets. Y-junctions yield smaller droplets than T-junctions and only the flow rate of the continuous phase needs to be controlled for monodisperse emulsification.[10] In contrast, for T-junctions both flow rates need to be controlled.[13] A complication for parallelizing Y-junctions is the fact that two connections are needed to introduce both liquids. Thus, especially designs d and e seem suitable for mass parallelization, as more oil channels can be positioned around one continuous-phase channel, leading to an area-efficient design (see Figure 4).

Acknowledgments

The authors wish to thank Amal Sawalha and Anja Warmerdam for performing part of the experiments, Michael van Ginkel for writing the droplet analysis script, and MicroNed for supporting this research.

Literature Cited

1. De Menech M, Garstecki P, Jousse F, Stone HA. Transition from squeezing to dripping in a microfluidic T-shaped junction. *J Fluid Mech*. 2008;595:141–161.
2. Garstecki P, Fuerstman MJ, Stone HA, Whitesides GM. Formation of droplets and bubbles in a microfluidic T-junction - scaling and mechanism of break-up. *Lab Chip*. 2006;6:437–446.
3. Graaf Svd, Nisisako T, Schroën CGPH, Sman RGMvd, Boom RM. Lattice Boltzmann simulations of droplet formation in a T-shaped microchannel. *Langmuir*. 2006;22:4144–4152.
4. Nisisako T, Torii T. Microfluidic large-scale integration on a chip for mass production of monodisperse droplets and particles. *Lab Chip*. 2008;8:287–293.
5. Thorsen T, Roberts RW, Arnold FH, Quake SR. Dynamic pattern formation in a vesicle-generating microfluidic device. *Phys Rev Lett*. 2001;86:4163–4166.
6. Xu JH, Li SW, Tan J, Luo GS. Correlations of droplet formation in T-junction microfluidic devices: From squeezing to dripping. *Microfluid Nanofluid*. 2008;5:711–717.
7. Capretto L, Mazzitelli S, Balestra C, Tosi A, Nastruzzi C. Effect of the gelation process on the production of alginate microbeads by microfluidic chip technology. *Lab Chip*. 2008;8:617–621.
8. Kawai A, Matsumoto S, Kiriya H, Oikawa T, Hara K, Ohkawa T, Futami T, Katayama K, Nishizawa K. Development of a microreactor for manufacturing gel particles without glass selection of diameter. *TOSOH Res Technol Rev*. 2003;47:3–9.
9. Kubo A, Shinmori H, Takeuchi T. Atrazine-imprinted microspheres prepared using a microfluidic device. *Chem Lett*. 2006;35:588–589.
10. Steegmans MLJ, Schroën CGPH, Boom RM. Characterization of emulsification at flat microchannel Y-junctions. *Langmuir*. 2009;25:3396–3401.
11. Benjamins J, Cagna A, Lucassen-Reynders EH. Viscoelastic properties of triacylglycerol/water interfaces covered by proteins. *Colloids Surf A*. 1996;114:245–254.
12. Graaf Svd, Steegmans MLJ, Sman RGMvd, Schroën CGPH, Boom RM. Droplet formation in a T-shaped microchannel junction: A model system for membrane emulsification. *Colloids Surfaces A*. 2005;266:106–116.
13. Nisisako T, Torii T, Higuchi T. Droplet formation in a microchannel network. *Lab Chip*. 2002;2:24–26.
14. Steegmans MLJ, Schroën CGPH, Boom RM. Generalised insights in droplet formation at T-junctions through statistical analysis. *Chem Eng Sci*. 2009;64:3042–3050.

Manuscript received Apr. 14, 2009, revision received July 20, 2009, and final revision received Sep. 23, 2009.